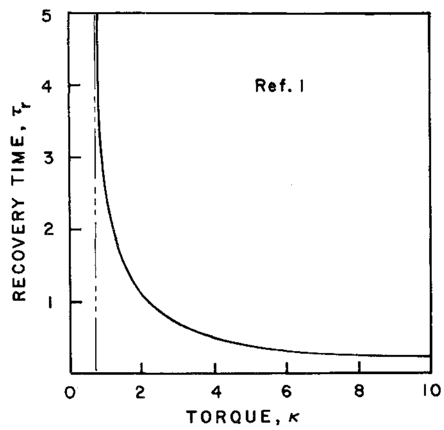

Fig. 1 Nondimensional recovery torque vs nondimensional recovery time (from Ref. 1).

Flat spin recovery of a spacecraft is thus equivalent to the process of driving a simple pendulum from rest at $\phi = 0$.

An integration of Eq. (7) for the case of a constant applied torque gives

$$\tfrac{1}{2}\phi'^2 = \kappa\phi + \cos\phi - 1 \tag{10}$$

for the stated initial conditions.

Pendulum motion not restricted to the neighborhood of $\phi = 0$ and spacecraft motion not restricted to the neighborhood of pure spin about the third axis require values for κ that produce real velocities ϕ' for all ϕ. The smallest such value represents the minimum nondimensional torque required for flat-spin recovery. This value is given in Ref. 1.

$$\kappa > 0.7246 \tag{11}$$

Substitution of the right-hand side of Eq. (8) into inequality (11) leads to the condition on flat spin recovery torque

$$T > 0.3623(C-B)\Omega^2\sqrt{\frac{C(C-A)}{B(B-A)}} \tag{12}$$

Inequality (12) differs from inequality (19) of Ref. 1 by the multiplicative radical. The radical did not appear in Ref. 1 because of the assumption that ω_2 and ω_3 have the same magnitude. The actual magnitudes of these rates are shown here in Eqs. (4). Omission of the multiplicative radical in inequality (12) can lead to a significant error in a recovery-torque determination for spacecraft having significantly different maximum and intermediate moments of inertia.

Figure 3 of Ref. 1 illustrates the time for which a given torque κ must act to produce a successful recovery. This figure is reproduced here as Fig. 1 for completeness. The nondimensional time shown is related to real time by the second of substitutions (6).

After the appropriate recovery impulse has been applied, spacecraft motion will have been transformed into spin about the first axis combined with nonzero rates ω_2 and ω_3. Once this state has been attained, active attitude control, a feature not included in the present model, may be engaged to remove the latter rates in order to produce pure spin about the first axis.

References

[1] Barba, P. M., Furumoto, N., and Leliakov, I. P., "Techniques for Flat-Spin Recovery of Spinning Satellites," AIAA Paper 73-859, Key Biscayne, Florida, Aug. 1973.

[2] Kaplan, M. H. and Patterson, T. C., "Attitude Acquisition Maneuvers for Bias Momentum Satellites," *COMSAT Technical Review,* Vol. 6, Spring 1976, pp. 1-23.

[3] Barba, P. M. and Aubrun, J. N., "Satellite Attitude Acquisition by Momentum Transfer," *AIAA Journal,* Vol. 14, Oct. 1976, pp. 1382-1386.

[4] Gebman, J. R. and Mingori, D. L., "Perturbation Solution for the Flat-Spin Recovery of Dual-Spin Spacecraft," *AIAA Journal,* Vol. 14, July 1976, pp. 859-867.

Analytic Steady-State Accuracy Solutions for Two Common Spacecraft Attitude Estimators

R. L. Farrenkopf*
TRW Defense and Space Systems Group, Redondo Beach, Calif.

Introduction

THIS Note treats the following two attitude estimation problems:

1) The single-axis attitude of a spacecraft is estimated by integrating the output of a rate gyro corrupted by drift rate and zero mean additive white Gaussian noise. The gyro drift rate fails to remain constant, its time derivative also behaving as a zero mean white noise process. Every T seconds, an attitude sensor (e.g., star tracker) measures the spacecraft attitude, and this information is utilized by an optimal estimator (i.e., Kalman filter) to update both the spacecraft attitude and the gyro drift rate. This attitude measurement also is corrupted by zero mean noise. Assuming that the estimator has converged to steady-state operation, what are the standard deviations of the attitude and gyro drift rate estimation errors just prior to, and also just after an attitude update?

2) The single-axis attitude of a spacecraft is measured every T seconds by an attitude sensor (e.g., earth sensor) that is corrupted by zero mean noise. Attitude and attitude rate estimates between samples are provided by a dynamic model of the spacecraft's angular motion, making use of the estimated control and disturbance torques acting upon the spacecraft. These torque estimates are generally imperfect, and, as a result, it is assumed that the true vehicular acceleration differs from its estimate by a zero mean Gaussian white noise process. An optimal estimator compensates these modeling errors by updating both the attitude estimate and its rate subsequent to each attitude measurement sample. Assuming that the estimator has converged to steady-state operation, what are the standard deviations of the attitude and rate estimation errors just prior to a measurement update? Similarly, what are these errors just subsequent to such an update?

It will be shown that the analytic representation of problem 2 is similar to that of problem 1. The latter was considered first by the author in Ref. 1, in which graphical results were presented. Since then, a complete analytic solution has been discovered, and this will be presented in what follows.

Problem Solution

Problem 1

It is assumed that the relatively fixed gyro error sources (e.g., scale factor) can be calibrated by an appropriate

Presented as Paper 74-903 at the AIAA Mechanics and Control of Flight Conference, Anaheim, Calif., Aug. 5-9, 1974; submitted Aug. 9, 1974; revision received Jan. 4, 1978.

Index categories: Spacecraft Systems; Spacecraft Dynamics and Control; Spacecraft Navigation, Guidance, and Flight-Path Control.

*Senior Staff Engineer, Systems Engineering.

spacecraft maneuver profile. No generality then is lost by assuming that the spacecraft attitude rate $\dot{\theta}$ is related to the gyro output ω_m by

$$\dot{\theta}=\omega_m - w - n_v \quad (1)$$

where w is the gyro drift rate, and n_v represents zero mean white Gaussian noise whose autocorrelation function satisfies

$$E[n_v(t)n_v(\tau)]=\sigma_v^2\delta(t-\tau) \quad (2)$$

where $\delta(t)$ is the Dirac delta function. The drift rate is assumed to satisfy

$$\dot{w}=n_u \quad (3)$$

where n_u is zero mean white Gaussian noise, given by

$$E[n_u(t)n_u(\tau)]=\sigma_u^2\delta(t-\tau) \quad (4)$$

Estimates of $\dot{\theta}$ and $\dot{w}$ are formed by taking expectations of Eqs. (1) and (3), respectively. Letting the caret denote "the expected value of" and noting the zero mean character of the gyro noise sources, it follows that the estimates are

$$\hat{\dot{\theta}}=\omega_m - \hat{w} \quad (5)$$

$$\hat{\dot{w}}=0 \quad (6)$$

It is now a straightforward matter to show that

$$\begin{bmatrix} \theta-\hat{\theta} \\ w-\hat{w} \end{bmatrix}_{t_{i+1}} = \Phi \begin{bmatrix} \theta-\hat{\theta} \\ w-\hat{w} \end{bmatrix}_{t_i} + \begin{bmatrix} f_{i+1} \\ g_{i+1} \end{bmatrix} \quad (7)$$

where Φ is the state transition matrix:

$$\Phi=\begin{bmatrix} 1 & -T \\ 0 & 1 \end{bmatrix} \quad (8)$$

where $T=t_{i+1}-t_i$, and

$$f_{i+1}=\int_{t_i}^{t_{i+1}} [-n_v(s)-(t_{i+1}-s)n_u(s)]\,ds \quad (9)$$

$$g_{i+1}=\int_{t_i}^{t_{i+1}} n_u(s)\,ds \quad (10)$$

The state noise covariance matrix Q can be computed as

$$Q=\begin{bmatrix} E[f_{i+1}^2] & E[f_{i+1}g_{i+1}] \\ E[f_{i+1}g_{i+1}] & E[g_{i+1}^2] \end{bmatrix} = \begin{bmatrix} \sigma_v^2 T + \tfrac{1}{3}\sigma_u^2 T^3 & -\tfrac{1}{2}\sigma_u^2 T^2 \\ -\tfrac{1}{2}\sigma_u^2 T^2 & \sigma_u^2 T \end{bmatrix} \quad (11)$$

and is independent of i for the fixed update intervals assumed.

The attitude sensor measurement y_{i+1} at t_{i+1} is clearly

$$y_{i+1}=\theta_{i+1}+n_{i+1} \quad (12)$$

when n represents the zero mean noise satisfying

$$E[n_i\, n_j]=\begin{cases} \sigma_n^2 & ; j=i \\ 0 & ; j\neq i \end{cases} \quad (13)$$

Forming $\hat{y}_{i+1}$ using Eq. (12), it follows that the measurement residual at t_{i+1} is

$$y_{i+1}-\hat{y}_{i+1}=M\begin{bmatrix} \theta-\hat{\theta} \\ w-\hat{w} \end{bmatrix}_{t_{i+1}} + n_{i+1} \quad (14)$$

where M is the measurement matrix:

$$M=[1 \quad 0] \quad (15)$$

The measurement noise covariance matrix is simply the scalar

$$R=E[n_{i+1}^2]=\sigma_n^2 \quad (16)$$

It now is assumed that attitude sensor/Kalman filter updates are provided at $t_1, t_2, \ldots$. A measure of the filter's estimation error just prior to an update is provided by the components of the 2×2 matrix:

$$S_i \triangleq S(t_i) \triangleq \{s_{ij}(t_i)\} = E\{[\theta-\hat{\theta}, w-\hat{w}]^T[\theta-\hat{\theta}, w-\hat{w}]\} \quad (17)$$

evaluated at t_i-. Similarly, the improved estimate just subsequent to an update is provided by the matrix

$$P_i \triangleq P(t_i) \triangleq \{p_{ij}(t_i)\} = E\{[\theta-\hat{\theta}, w-\hat{w}]^T[\theta-\hat{\theta}, w-\hat{w}]\} \quad (18)$$

evaluated at t_i+. Having defined these error covariance matrices and the system matrices Φ, Q, M, and R, the standard Kalman filter sequential equations now can be written defining the system's estimated error propagation:

$$S_{i+1}=\Phi P_i \Phi^T + Q \quad (19)$$

$$K_{i+1}=S_{i+1}M^T\{MS_{i+1}M^T+R\}^{-1} \quad (20)$$

$$P_{i+1}=S_{i+1}-K_{i+1}M\,S_{i+1} \quad (21)$$

Now the steady-state condition will be imposed, namely,

$$P_{i+1}=P_i, \qquad S_{i+1}=S_i \quad (22)$$

Noting the symmetry of the 2×2 matrices P and S, Eqs. (19-22) now yield six independent relations regarding their components. From these, a single quartic equation in s_{12} can be derived.[1] Defining

$$x=T\,s_{12}/\sigma_n^2 \quad (23)$$

$$S_v=\sigma_v T^{1/2}/\sigma_n \quad (24)$$

$$S_u=\sigma_u T^{3/2}/\sigma_n \quad (25)$$

this quartic can be written as

$$x^4+S_u^2x^3+S_u^2[(1/6)S_u^2-S_v^2-2]x^2+S_u^4x+S_u^4=0 \quad (26)$$

An analytic solution for this quartic now has been found with the discovery that it is a product of the two quadratics

$$x^2+[(S_u^2/2)\pm\beta]x+S_u^2=0 \quad (27)$$

where

$$\beta=+[S_u^2(4+S_v^2)+(S_u^4/12)]^{1/2} \quad (28)$$

The root of physical significance is the maximally negative root assuming $+\beta$ in Eq. (27). Thus,

$$x=-\frac{1}{2}\left[\left(\frac{S_u^2}{2}+\beta\right)+\sqrt{\left(\frac{S_u^2}{2}+\beta\right)^2-4S_u^2}\right] \quad (29)$$

The six equations formed from Eqs. (19-22) now yield the final result

$$\sigma_\theta(-)=\sqrt{s_{11}}=\sigma_n\sqrt{\left(\frac{x}{S_u}\right)^2-1} \tag{30†}$$

$$\sigma_\theta(+)=\sqrt{p_{11}}=\sigma_n\sqrt{1-\left(\frac{S_u}{x}\right)^2} \tag{31}$$

$$\sigma_w(-)=\sqrt{s_{22}}=\frac{\sigma_n}{T}\sqrt{S_u^2\left(\frac{1}{x}+\frac{1}{2}\right)-x} \tag{32}$$

$$\sigma_w(+)=\sqrt{p_{22}}=\frac{\sigma_n}{T}\sqrt{S_u^2\left(\frac{1}{x}-\frac{1}{2}\right)-x} \tag{33}$$

Problem 2

This system has no gyro, obtaining its attitude and attitude rate estimates by means of a dynamic model. The single-axis spacecraft motion is described by

$$\dot{\theta}=w \tag{34}$$

$$\dot{w}=u \tag{35}$$

where w is its angular velocity and u is the torque acting upon the spacecraft. Taking estimates of $\dot{\theta}$, $\dot{w}$, and u in the preceding equations, it follows that

$$\begin{bmatrix}\theta-\hat{\theta}\\ \hat{w}-w\end{bmatrix}_{t_{i+1}}=\Phi\begin{bmatrix}\theta-\hat{\theta}\\ \hat{w}-w\end{bmatrix}_{t_i}+\begin{bmatrix}f_{i+1}\\ g_{i+1}\end{bmatrix} \tag{36}$$

which is the same as Eq. (7) except for the interchange in the positions of w and $\hat{w}$, and in which f_{i+1} and g_{i+1} are given by Eqs. (9) and (10) under the restrictions $n_v=0$, $n_u=\hat{u}-u$. Subsequent analysis is now identical to problem 1, with Eqs. (28-33) again providing a recipe for obtaining steady-state performance. Here S_v is taken equal to zero, and S_u is given by Eq. (25), noting also Eq. (4). This completes the steady-state performance description of these two common spacecraft attitude estimators.

Example

A problem 1 type of attitude estimator updates its gyro every 600 s using a star tracker for which $\sigma_n=20$ arc-s. The gyro, as a component, behaves such that, statistically, its drift rate changes 10^{-2} arc-s/s(1σ) in 12 h, whereas its integrated output changes 8.75 arc-s (1σ) in 0.5 h. What is the steady-state behavior of this estimator?

The Q matrix of Eq. (11) shows the gyro impact on attitude and drift rate for any time interval. σ_u is obtained from the drift rate specification, i.e.,

Source Eq.

$$\sigma_u^2(12\times3600)=(10^{-2})^2 \quad \therefore \quad \sigma_u=4.81\times10^{-5}\text{arc-s/s}^{3/2} \tag{11}$$

$$\sigma_v^2(0.5\times3600)+\tfrac{1}{3}\sigma_u^2(0.5\times3600)^3$$
$$=(8.75)^2 \quad \therefore \quad \sigma_v=0.200\text{ arc-s/s}^{1/2} \tag{11}$$

$$S_v=(0.2)(600)^{1/2}/20=0.245 \tag{24}$$

$$S_u=(4.8\times10^{-5})(600)^{1.5}/20=0.035 \tag{25}$$

$$\beta=0.07122 \tag{28}$$

$$x=-0.04234 \tag{29}$$

†When $S_u=0$, take $x/S_u=-\tfrac{1}{2}[S_v+\sqrt{S_v^2+4}]$.

The steady-state behavior now follows:

$$\sigma_\theta(-)=13.2\text{ arc-s} \tag{30}$$

$$\sigma_\theta(+)=11.0\text{ arc-s} \tag{31}$$

$$\sigma_w(-)=0.0039\text{ arc-s/s} \tag{32}$$

$$\sigma_w(+)=0.0037\text{ arc-s/s} \tag{33}$$

References

[1]Farrenkopf, R.L., "Generalized Results for Precision Attitude Reference Systems Using Gyros," AIAA Paper 74-903, Anaheim, Calif., Aug. 1974.

[2]Sorenson, H.W., "Kalman Filtering Techniques," *Advances in Control Systems,* Vol. 3, Academic Press, New York, 1966, pp. 219-292.

Optimal Flare in Presence of Wind Shears

Bohdan G. Kunciw*
Air Force Flight Dynamics Laboratory, Wright-Patterson Air Force Base, Ohio

Introduction

INVESTIGATIONS of several aircraft accidents indicate that wind shear is a factor that can cause aircraft crashes. The "Speckled Trout" C-135A advanced automatic landing flight-test program at the Air Force Flight Dynamics Laboratory included a hybrid simulation of the aircraft and automatic control system to investigate the effects of wind shear.[1] This study indicated that a logarithmically decreasing headwind from 50.67 ft/s (30 knots) at 510 ft AGL (above ground level) to 0 ft/s at 10 ft AGL resulted in an automatic landing 721 ft short of the no-wind case and a sink rate at touchdown of −6.2 ft/s instead of −2.1 ft/s for the no-wind case. From an altitude of 1000 to 510 ft, the wind was a constant 50.67 ft/s. This particular wind shear condition resulted in the worst performance compared to steady-state winds and linear shears of comparable magnitude. (Logarithmic winds were considered more representative of atmospheric conditions.) Considering the preceding logarithmic shear, a similar 30-knot headwind shear that is linear, and a constant 30-knot headwind, the longitudinal range dispersion at touchdown was 2017 ft, and the sink rate dispersion at touchdown was 5.55 ft/s. Dispersion is the span from the minimum to the maximum values; each extreme limit is determined by a wind condition. The longitudinal control equations were based on the conventional operational autopilot installed in the aircraft; during the time-based exponential flare, the throttles retard linearly.

The objective of this investigation is to design a flare control law that will enable an aircraft on automatic approach in the presence of unknown wind shears to achieve the smallest possible longitudinal dispersion and sink rate deviation at touchdown relative to a no-wind case. The flare portion of the automatic landing was chosen, since the flare control law is a major cause of poor landings in the presence of wind shears.[1]

The best possible performance should be obtained by using optimal control theory. Nonlinear equations of motion

Received April 4, 1977; revision received Feb. 2, 1978.

Index categories: Guidance and Control; Landing Dynamics.

*Presently Instructor, Air Force Test Pilot School, Edwards Air Force Base, Calif. Member AIAA.